Oxidative Metabolism of Pyruvate Is Required for Meiotic Maturation of Murine Oocytes In Vivo[1]

Mark T. Johnson,[2,5,6] Edward A. Freeman,[3,5] David K. Gardner,[6] and Patricia A. Hunt[4,5]

Department of Genetics,[5] Case School of Medicine, Case Western Reserve University, Cleveland, Ohio 44106
Colorado Center for Reproductive Medicine,[6] Englewood, Colorado 80110

ABSTRACT

The requirement for oxidative metabolism of pyruvate during oogenesis in vivo was evaluated by inactivating *Pdha1*, a gene encoding an enzymatic subunit of pyruvate dehydrogenase complex, in murine oocytes at the beginning of the follicular growth phase. Immunohistochemical analysis revealed that *Pdha1⁻* oocytes have dramatically reduced amounts of pyruvate dehydrogenase enzyme by the secondary follicle stage. Despite this reduction, these oocytes grow to normal size, are ovulated, and can be fertilized. *Pdha1⁻* oocytes are, however, impaired in their ability to support embryonic development, as demonstrated by the failure of fertilized oocytes to develop beyond the one-cell zygote stage in vivo. Immunocytochemical evaluation showed that almost all (98.4%) ovulated *Pdha1⁻* oocytes have not completed meiotic maturation and/or have gross abnormalities of the meiotic spindle and chromatin. Meiotic maturation is even more compromised when these oocytes are matured in vitro in the absence of cumulus cells or in the presence of the gap junction inhibitor 18-alpha glycyrrhetinic acid, indicating that cumulus cells can partially compensate for this enzymatic deficiency through a gap junction-mediated mechanism. Ovulated *Pdha1⁻* oocytes were also shown to have reduced levels of total ATP content and NAD(P)H autofluorescence relative to oocytes without this enzymatic deficiency. These studies demonstrate that oxidative metabolism of pyruvate is essential for proper completion of oogenesis, serving as a vital source of energy during meiotic maturation. At earlier stages of oogenesis this metabolic pathway may not be necessary due to metabolic compensation by the granulosa cells.

embryo, gamete biology, granulosa cells, meiosis, meiotic maturation, mitochondria and metabolism, oocyte development, oogenesis, pyruvate

INTRODUCTION

During oogenesis in mammals, the oocyte grows by more than two orders of magnitude, produces large quantities of myriad macromolecules, and undergoes a complex series of morphologic and developmental changes [1]. Clearly, these developmental processes exact a tremendous energetic toll. The oocyte must meet its energetic requirements during development by modulating a number of metabolic pathways that generate ATP. For the last several decades there has been considerable interest in pyruvate as an energy source for developing oocytes. The focus on pyruvate originated with the observation that murine oocytes denuded of surrounding cumulus cells could complete meiotic maturation—the latter stage of oogenesis in which meiosis is resumed and the oocyte prepares for ovulation—in culture media containing pyruvate, but not glucose or lactate [2]. Subsequent studies in vitro demonstrated that throughout oogenesis, oocytes metabolize pyruvate oxidatively through mitochondrial oxidative metabolic pathways, yielding ATP and CO_2 [3, 4]. The importance of mitochondrial metabolism during oogenesis was further supported by the observation that rat oocytes cultured in vitro cannot complete meiotic maturation in either the absence of oxygen or the presence of inhibitors or uncouplers of mitochondrial oxidative phosphorylation [5]. Alternately, observations that both mitochondria are structurally immature throughout oogenesis and follicles grow to the preovulatory stage in the presence of malonate, an inhibitor of the mitochondrial tricarboxylic acid cycle, indicate that mitochondrial metabolism may not be required during oogenesis [6, 7].

In considering how oocytes are supported energetically, the oocyte cannot be considered in isolation, as it is both physically and metabolically linked to the surrounding granulosa cells. The oocyte is connected via gap junctions to granulosa cells until just prior to ovulation [8]. Granulosa cells supply the oocyte with ATP and energy-producing substrates, such as glucose [9, 10]. This metabolic cooperativity is highly dynamic: oocytes can upregulate flux through glycolysis and the citric acid cycle by several-fold in cumulus cells through paracrine signaling [11]. When oocytes are enclosed in cumulus cells, they can complete meiotic maturation in the absence of exogenous pyruvate, provided that glucose is present in the media. It has been proposed that cumulus cells supply the oocyte with pyruvate by metabolizing glucose through glycolysis, but alternative explanations, such as the provision of ATP or other substrates, cannot be excluded [12]. From the described metabolic studies, it remains unclear whether oocytes require oxidative metabolism of pyruvate to complete development in vitro. The importance of this metabolic pathway during development in vivo is even less clear, since the metabolism observed in vitro may not reflect that which occurs in vivo for a number of reasons.

To determine whether oxidative metabolism of pyruvate is required during oogenesis in vivo, we have used a genetic approach in these studies to block this metabolic pathway in developing oocytes. Specifically, a mutation that inactivates pyruvate dehydrogenase complex (PDC), the mitochondrial multienzyme complex that catalyzes the first step in the oxidative metabolism of pyruvate, was introduced into oocytes at the beginning of the growth phase of oogenesis. During the

[2]Correspondence: Mark T. Johnson, Colorado Center for Reproductive Medicine, 799 East Hampden Ave., Suite 520, Englewood, CO 80110. FAX: 303 744 0688; e-mail: mtj@case.edu
[3]Current address: Department of Biology, St. John Fisher College, Rochester, NY 14618.
[4]Current address: School of Molecular Biosciences, Washington State University, Pullman, WA 99164.

2- to 3-wk growth phase, the murine oocyte undergoes a period of rapid growth and development to attain full size and maturational competence. By analyzing the development of oocytes in which a PDC gene has been inactivated, we have established the importance of pyruvate during meiotic maturation in vivo.

MATERIALS AND METHODS

Animals and Breeding Scheme

Procedures for the maintenance of animal colonies and all experiments performed on mice were approved by the Institutional Animal Care and Use Committees of Case Western Reserve University and the Health One Alliance. Animals carrying an inducible, targeted mutation in the X-linked pyruvate dehydrogenase E1 alpha 1 gene (designated $Pdha1^{flox}$) were obtained from Dr. Mulchand Patel, University of Buffalo, Buffalo, NY [13]. In the presence of the Cre recombinase, two loxP sites inserted into introns of this gene are catalyzed to recombine, leading to a null mutation in which exon 8 is deleted [13]. A Cre recombinase transgene driven by the zona pellucida *protein-3* gene promoter (*Zp3-Cre*) was used to restrict expression of the recombinase to oocytes [14]. The *Zp3-Cre* transgene has been shown to be expressed in oocytes beginning at the growth phase and to catalyze recombination between loxP sites efficiently [14, 15]. A two-step breeding strategy was devised to inactivate *Pdha1* in developing oocytes. First, females homozygous for the $Pdha1^{flox}$ mutation were bred with males that carried a *Zp3-Cre* transgene. Male offspring that carried the $Pdha1^{flox}$ mutation and the *Zp3-Cre* transgene then were bred with females homozygous for the $Pdha1^{flox}$ allele. All resulting female progeny were homozygous for the $Pdha1^{flox}$ mutation. Those that carried the *Zp3-Cre* transgene were considered experimental animals (abbreviated $Pdha1^-$), whereas littermates that lacked the transgene served as control animals (abbreviated $Pdha1^+$).

Histology and Immunohistochemistry

Ovaries were dissected from killed $Pdha1^-$ and $Pdha^+$ mice at 1, 2, 3, and 12 mo of age. For general histologic analysis, samples were fixed in Bouin fixative overnight and then paraffin embedded, sectioned, and stained with hematoxylin-eosin. For immunohistochemical analysis, sections were deparaffinated, rehydrated, and subjected to antigen retrieval by incubation in 10 mM sodium citrate with 0.05% Tween 20 at 100°C for 20 min. A rabbit polyclonal antibody raised against either human pyruvate dehydrogenase (PDH; 1:1000 dilution) or human dihydrolipoamide dehydrogenase (DLD; 1:1000) was used as a primary antibody (kindly provided by Dr. Mulchand S. Patel). A fluorescein-conjugated goat anti-rabbit monoclonal antibody (Invitrogen) served as the secondary antibody (1:200 dilution). Following washes, nuclei were counterstained with 4′,6′-diamidino-2-phenylindole (DAPI; Sigma) and subjected to epifluorescence microscopy using appropriate filter sets for fluorescein isothiocyanate (FITC) and DAPI.

Superovulation and Immunocytochemical Evaluation of Oocytes

Female mice aged 4–5 wk were injected intraperitoneally with 2.5 IU eCG, and then were injected 48 h later with 5 IU hCG (Sigma). Ovulated oocytes were collected from the ampullae at 13–15 h after the second injection. Cumulus cells were removed by incubating briefly in 1 mg/ml hyaluronidase. Oocytes were evaluated using a dissecting scope, and images were captured using a Spot RT-SE CCD camera, with measurements being performed using Spot software (Diagnostic Instruments). Immunocytochemical evaluation of oocytes fixed in fibrin clots was performed as described by Hodges et al. [16] using an FITC-conjugated anti-tubulin monoclonal antibody (Sigma) and DAPI. For evaluation of double-stranded breaks of genomic DNA, fixed oocytes were subjected to TUNEL using the TMR-fluorophore-based kit (Roche) with described positive and negative controls. Samples were ultimately evaluated using epifluorescence microscopy.

Collection of Embryos Fertilized In Vivo

Following the previously described superovulation regimen, females were immediately mated with C57Bl/6 males that were proven to be fertile. To evaluate fertilization, zygotes were collected from the ampullae at 16 h after hCG and mating and were incubated in 0.5 μg/ml of the nuclear stain Hoechst 33342 (Sigma) for 30 min [17]. Stained nuclei were visualized with a DAPI filter set. To evaluate embryonic development, embryos were collected at 28–30 h and visualized under a dissecting scope.

Collection of Germinal Vesicle Stage Oocytes and In Vitro Maturation

Female mice aged 28 ± 2 days were primed with 2.5 IU eCG and then killed 48 h following the injection. Ovaries were removed and were placed in collection media containing Waymouth MB 752/1 Media with L-glutamine (Invitrogen) supplemented with 10% fetal bovine serum (Gibco) and 0.23 mM pyruvate [18]. Antral follicles were punctured to release cumulus-oocyte complexes (COCs). For analysis of germinal vesicle-stage (GV-stage) oocytes or for in vitro maturation requiring denuded oocytes, cumulus cells were removed by brief exposure to 1 mg/ml hyaluronidase followed by mechanical removal. Immature GV-stage oocytes were fixed and stained with DAPI as described previously and were categorized based on their chromatin morphology [19].

To mature GV-stage oocytes in vitro, oocytes either surrounded by or denuded of cumulus cells were incubated for 16–18 h in collection media maintained in ambient air supplemented with 5% CO_2 at 37°C [18]. For inhibiting gap junctional communications between cumulus cells and the oocyte, 10 μM of 18-α glycyrrhetinic acid was added to the media, and 3 mg/ml polyvinylpyrrolidone (PVP; Sigma) was used in place of fetal bovine serum to prevent adsorption of the inhibitor to serum proteins. Previous studies have demonstrated that concentrations greater than 5 μM reduce cumulus cell-oocyte metabolic coupling by more than 98% [20]. As a control, oocytes were also matured in PVP-substituted collection media.

Assessment of Energy Status

Total ATP content in pools of 5–10 GVs and superovulated (SO) oocytes was determined using the bioluminescent somatic cell assay kit (Sigma) with modifications as described by Combelles and Albertini [21]. To assess the mitochondrial redox state, the autofluorescence of oocytes was determined for two different spectra reflecting redox status of two energy molecules: (1) NAD(P)H: 360/40 nm excitation and 480/40 nm emission, and (2) oxidized flavoproteins: 450/40 nm excitation and 535/40 nm emission. Images were captured, and average fluorescence of the entire oocyte was determined using Metafluor software (Molecular Devices). Studies have shown that these two fluorescent signals are in tight equilibrium and correlate with mitochondrial respiratory activity [22, 23]. Mitochondrial membrane potentials for oocytes were determined using the carbocyanine dye, JC-1 (5,5′,6,6′-tetrachloro-1,1,3,3′-tetraethylbenimidazoylcarbocyanine iodide), which accumulates in the mitochondria in a potential-dependent manner [24]. Following illumination using a 480/30 filter, fluorescence of the monomeric form of the dye was detected with a 535/40 filter, and J-aggregates were detected with a 580/40-nm filter. Results were presented as ratios of aggregate:monomeric fluorescence.

Data Statistics

For two-group comparisons of means, the Student *t*-test was performed. For comparisons of proportions, the Fisher exact test was performed for 2×2 tables and the chi-square test for larger contingency tables. For comparisons of multiple means, sample groups were tested for normality of distributions using the Kolmogorov-Smirnov test. Those data sets with normal distributions were analyzed by analyses of variance (ANOVA) followed by the Bonferroni correction for multiple testing. Those samples that did not pass the normality test were analyzed with the Kruskal-Wallis nonparametric test followed by Dunn post-test.
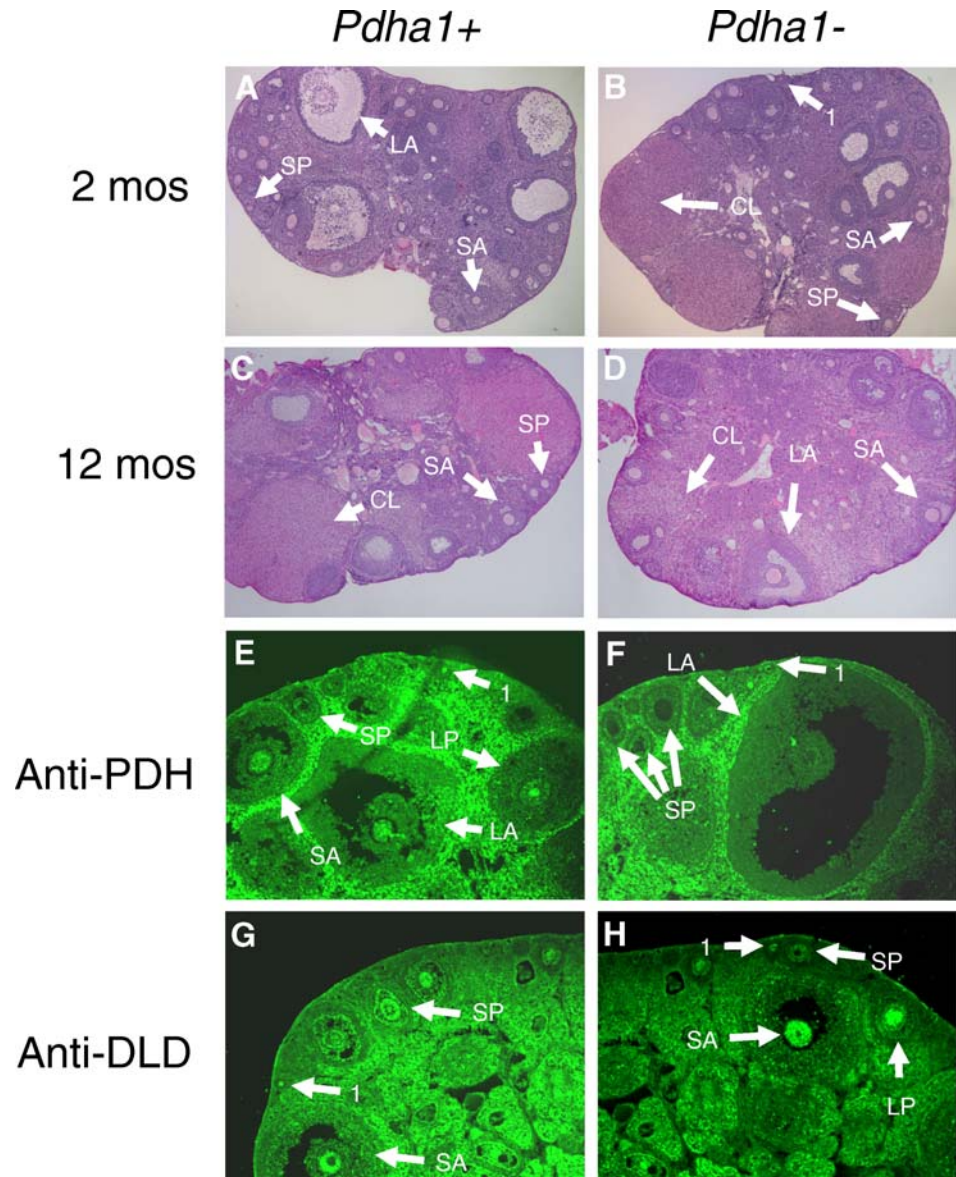
RESULTS

Pdha1− females Are Sterile but Have Histologically Normal Ovaries

Ten females that carried the *Zp3-Cre* transgene (*Pdha1−* females) were bred with males proven to be fertile for a cumulative period of 60 mo. No progeny or overt signs of pregnancy were observed from *Pdha1−* females.

Ovaries from *Pdha1−* females were compared to those from littermates lacking the transgene (*Pdha1+* females). Ovaries from *Pdha1−* animals were grossly and histologically indistinguishable (Fig. 1, A–D) from control littermates at all four ages examined (4, 8, and 12 wk, and 10 mo). Of note, ovaries from

FIG. 1.   Histologic and immunohistologic analysis of ovaries. Ovaries containing *Pdha1⁻* and control oocytes were collected at 2 mo (**A**, **B**, **E–H**) and 12 mo (**C**, **D**). Samples were stained with hematoxylin-eosin for histologic evaluation (**A–D**). Samples were stained with anti-PDH (**E**, **F**) or anti-DLD (**G**, **H**) primary antibodies for immunohistologic analysis. Follicles of different developmental stages are marked as follows: 1, primary; SP, small preantral; LP, large preantral; SA, small antral; LA, large antral. Original magnification ×40.

Pdha1⁻ animals had follicles in all stages of development, and those from sexually mature animals had Graafian follicles and *corpora lutea*, suggesting that oocytes were ovulated. Measurements of oocyte diameters from Graafian follicles revealed no difference in oocyte size between the two genotypes (*Pdha1⁻*: 79.5 ± 7.5 μm, n = 11; *Pdha1⁺*: 76.7 ± 4.9 μm, n = 18; $P > 0.05$). Immunohistochemical analysis of ovaries from *Pdha1⁻* ovaries using an anti-PDH antibody could not detect PDH in most oocytes at the primary follicle stage, nor could it detect PDH in any oocytes at secondary follicle or subsequent stages of development (Fig. 1F). Primordial-stage oocytes and somatic cells, including the surrounding cumulus cells, had strong staining. In contrast, PDH was detected in all developmental stages of *Pdha1⁺* oocytes (Fig. 1E). The DLD protein, another catalytic component of PDC, was detected in all *Pdha1⁺* and *Pdha1⁻* oocytes (Fig. 1, G and H).

Pdha1⁻ Oocytes Have Maturational and Postfertilization Developmental Defects

Superovulation produced comparable numbers of *Pdha1⁻* oocytes relative to controls: 18.5 ± 12, (n = 19 stimulations) vs. 21.9 ± 8.7 (n = 22 stimulations), respectively. Although eggs were similar in size (*Pdha1⁺* diameter: 71.6 ± 4.1 μm, n = 483; *Pdha1⁻* diameter: 71.8 ± 3.3 μm, n = 351), significantly fewer *Pdha1⁻* oocytes had polar bodies (69% vs. 26%; $P < 0.001$). To evaluate the meiotic spindle and chromosomes, these eggs also were analyzed by immunocytochemistry as previously described [16]. Whereas most of the *Pdha1⁺* oocytes were at metaphase of meiosis I (MI) or meiosis II (MII), almost 90% of *Pdha1⁻* eggs had morphologies that were atypical of any developmental stage (Fig. 2). The abnormal oocytes were grouped into three distinct categories, which are believed to represent perturbation and arrest at different developmental stages (Fig. 2, D–F). The first group was characterized by highly condensed chromatin and absence of spindle structures. These abnormalities presumably represent cellular degeneration either at the GV stage or shortly after breakdown of the nuclear membrane (Fig. 2D). In the second class of abnormalities, which constituted the majority of *Pdha1⁻* oocytes, the chromatin was eccentrically located, with only occasional evidence of discrete chromosomes or clumps of chromatin (Fig. 2E). Additionally, microtubular structures were often present, although none had the normal bipolar
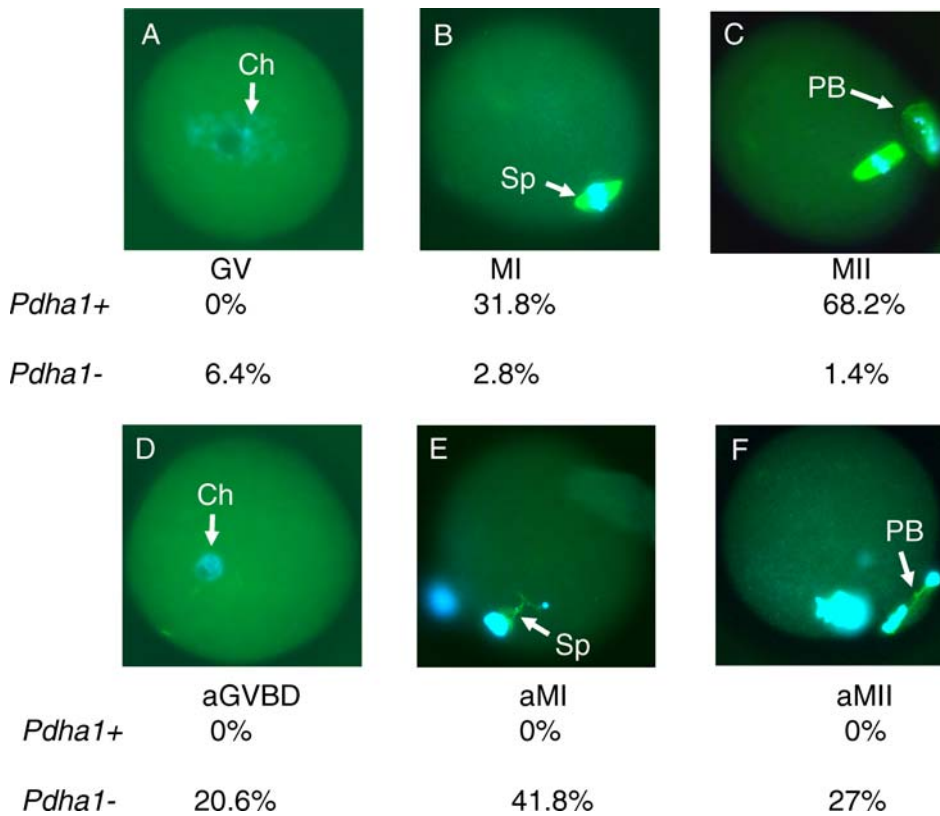
FIG. 2. Classification of SO $Pdha1^+$ and $Pdha1^-$ oocytes. Fixed oocytes were stained with an FITC-conjugated anti-β-tubulin antibody to visualize meiotic spindles (labeled Sp) and microtubular structures and DAPI to visualize chromatin (labeled Ch). **A–C**) Oocytes at different stages in the normal progression of meiotic maturation. **A**) GV. **B**) Metaphase I (MI). **C**) Metaphase II (MII, polar body marked PB). **D–F**) Oocytes with abnormal morphologies classified according to which developmental stage is perturbed or arrested. **D**) Abnormal germinal vesicle breakdown (aGVBD). **E**) Abnormal meiosis I (aMI). **F**) Abnormal meiosis II (aMII). The distributions of proportions are statistically different between $Pdha1^+$ and $Pdha1^-$ oocytes ($P < 0.01$). Original magnification ×400.

structure seen in control cells. Evidence of nuclear translocation and spindle formation, two processes that occur early in meiotic maturation, suggest that this group of oocytes has progressed further into meiosis I than the preceding class. The third group of $Pdha1^-$ oocytes had chromatin and spindle abnormalities similar to those seen in the second class, although polar bodies were identified (PB in Fig. 2F). The presence of a polar body indicates that these oocytes have completed the first meiotic division and entered meiosis II. TUNEL staining revealed that $Pdha1^-$ oocytes, regardless of chromatin morphology, rarely have evidence of double-stranded breaks indicative of apoptosis ($Pdha1^-$: 9.4% TUNEL positive, n = 64; $Pdha1^+$: 9.7% TUNEL positive, n = 31; $P >$ 0.1).

Collection of SO oocytes at 16 h after hCG and mating revealed that $Pdha1^-$ and $Pdha1^+$ oocytes were fertilized in vivo at similar rates ($Pdha1^-$: 51% fertilized, n = 51; $Pdha1^+$: 50.7% fertilized, n = 73; $P > 0.1$). However, collection at 28–30 h after hCG and mating revealed that none of the 158 $Pdha1^-$ zygotes had undergone the first cleavage division, whereas 25 of 68 $Pdha1^+$ embryos were at the two-cell stage ($P < 0.001$).

Dependence of Pdha1$^-$ *Oocytes on Cumulus Cells for Meiotic Maturation In Vitro*

Evaluation of chromatin conformation of GV-stage oocytes revealed that $Pdha1^-$ oocytes have a small but significantly decreased percentage of oocytes at the surrounded nucleolus (SN) stage, a developmentally more mature chromatin pattern in which the chromatin is tightly compacted around the nucleolus [19] ($Pdha1^+$: SN = 58%, n = 186; $Pdha1^-$: SN = 53%, n = 151; $P < 0.01$).

Comparison of $Pdha1^+$ oocytes matured in vitro within COCs to those matured in vivo revealed significantly higher proportions at the GV stage (15% vs. 0%, respectively),

although similar proportions of oocytes at the metaphase II indicate that conditions were sufficient to support in vitro maturation in the majority of oocytes (75.7% vs. 68.2%; Figs. 2 and 3A). COCs matured similarly in maturation media containing either fetal calf serum or PVP ($P > 0.05$; Fig. 3A).

When oocytes were denuded of surrounding cumulus cells (DNOs) for both genotypic classes, development was compromised relative to that seen with COCs (Fig. 3). The proportion of $Pdha1^-$ oocytes at the GV or abnormal GV breakdown (aGVBD) stage was significantly higher for DNOs than COCs (80% vs. 35%; $P < 0.001$), suggesting that a higher percentage arrested at earlier stages of maturation. In contrast, similar proportions of $Pdha1^+$ COCs and DNOs were classified as GV or aGVBD ($P > 0.1$).
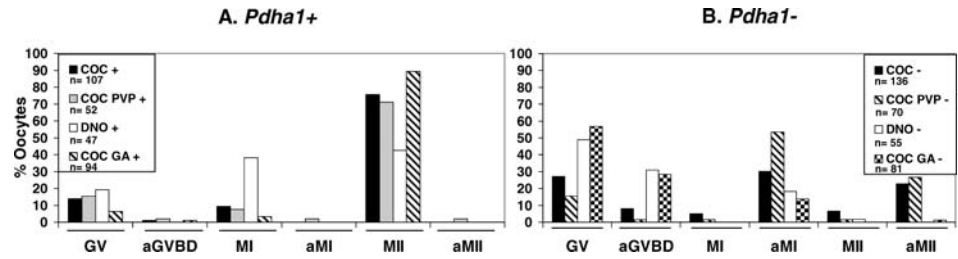
To determine whether the cumulus cell effect was mediated through gap junctions, $Pdha1^-$ oocytes enclosed in cumulus cells were cultured in the presence of the gap junction inhibitor, 18 α-glycyrrhetinic acid. Addition of the inhibitor also significantly decreased development of $Pdha1^-$ oocytes: 85% of oocytes remained at the GV or aGVBD stage compared with 35% or 17% for $Pdha1^-$ COCs matured in media containing fetal calf serum or PVP, respectively.

Energy Status of Pdha1$^-$ *Oocytes Worsens During Meiotic Maturation*

Superovulated (SO) $Pdha1^-$ oocytes were found to have significantly reduced levels of ATP relative to both $Pdha1^+$ oocytes at either the GV or SO stage and $Pdha1^-$ oocytes at the GV stage (Fig. 4A). In contrast, $Pdha1^+$ oocytes had similar ATP content at both developmental stages. In evaluating mitochondrial redox status by autofluorescence, it was found that the levels of NAD(P)H fluorescence were not significantly different between $Pdha1^+$ and $Pdha1^-$ oocytes at the GV stage (Fig. 4B). Following meiotic maturation and ovulation in vivo, NAD(P)H fluorescence had increased for both genotypic

FIG. 3. In vitro maturation of $Pdha1^+$ (**A**) and $Pdha1^-$ (**B**) oocytes. Culture conditions included COCs in standard collection medium (COC); COCs in PVP-substituted media (COC PVP); denuded oocytes in CM (DNO), and COCs matured in media containing 18-α glycyrrhetinic acid and PVP (COC GA).

classes, although the $Pdha1^-$ oocytes had not increased to a similar degree, resulting in significantly lower levels of fluorescence relative to $Pdha1^+$ SO oocytes. In evaluating flavoprotein fluorescence, it was found that $Pdha1^-$ oocytes had higher levels of fluorescence than $Pdha1^+$ oocytes at both the GV and SO stages, although the difference was much greater at the SO stage (Fig. 4C). Analysis of the mitochondrial membrane potential using the dye JC-1 revealed that $Pdha1^-$ oocytes had aggregate:monomer ratios similar to those in $Pdha1^+$ oocytes at the same developmental stage (Fig. 4D). Of note, SO oocytes of both genotypic classes had ratios that were higher than those at the GV stage. In examining the epifluorescent images, there were no appreciable differences between $Pdha1^-$ and control oocytes in terms of mitochondrial distribution. In summary, it appears that $Pdha1^-$ oocytes have markedly compromised mitochondrial energy production following in vivo maturation and ovulation.
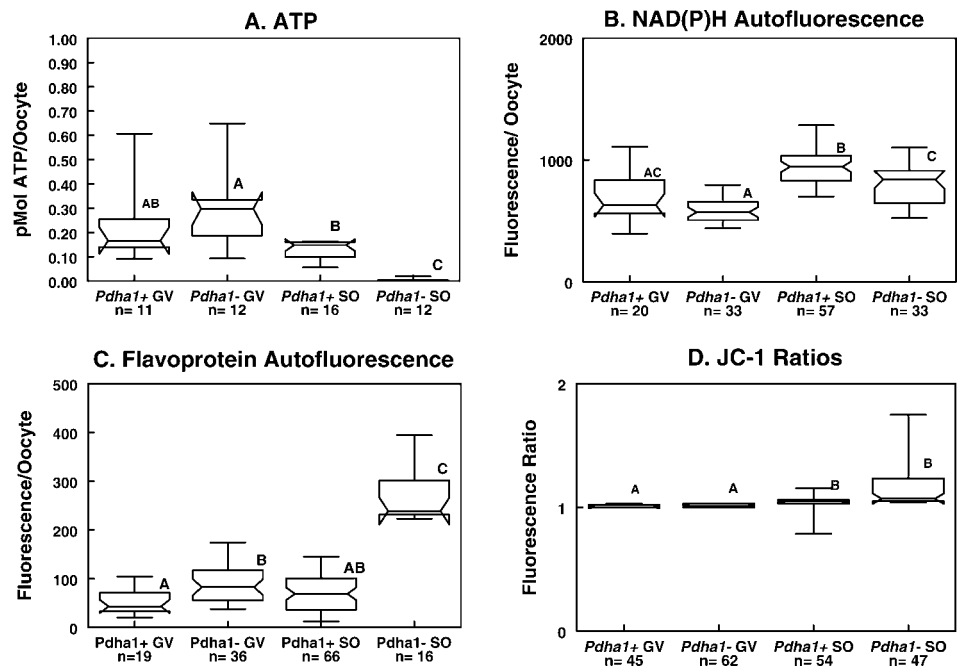
DISCUSSION

The Cre-loxP conditional mutation system was used to introduce a null mutation into the $Pdha1$ gene of oocytes at the initiation of the growth phase. Immunohistochemical analysis revealed that following induction of this mutation, PDH enzyme became substantially diminished by the secondary oocyte stage, which occurs within the first week of growth. Considering that the half-life of PDH may be as long as 2 days and the oocyte quadruples in size during the first week in the

growth phase, the concentration of enzyme in $Pdha1^-$ oocytes would be predicted to drop to less than 1% of that found in primordial oocytes over the first week of growth [25]. Although PDH is a heterotetrameric enzyme composed of two gene products, the lack of immunoreactivity following gene deletion was expected due to the instability of uncomplexed monomers, as has been reported for $Pdha1$-deficient embryonic stem cells [13]. The oocyte-specific nature of this mutation was shown by the presence of normal amounts of PDH immunoreactivity in surrounding cumulus cells (Fig. 1). Furthermore, PCR analysis of genomic DNA from cumulus cells surrounding $Pdha1^-$ oocytes from 10 different COCs detected no deletion in the $Pdha1$ gene (data not shown).

Oocytes deficient in PDC are uniformly incapable of completing meiotic maturation. This finding is consistent with previous studies demonstrating that denuded oocytes require pyruvate to complete meiotic maturation in vitro [2]. Without $Pdha1$, only a very small percentage of oocytes attain a normal metaphase II morphology using described immunocytochemical techniques (1.4%; Fig. 2C). It is likely that even these apparently normal oocytes are developmentally impaired based on the observation that none of 158 $Pdha1^-$ oocytes fertilized in vivo developed beyond the one-cell zygote stage. The phenotype of $Pdha1^-$ oocytes also demonstrates that meiotic maturation requires functional mitochondria. Mitochondrial dysfunction has been proposed as a factor in the increased incidence of aneuploidy in oocytes from older women. Of note,

FIG. 4. Box-whisker plots of results of energetic analyses of $Pdha1^-$ and control oocytes at the GV and SO stages. **A**) Total ATP (each sample was a group of 5–15 oocytes). **B**) NAD(P)H autofluorescence. **C**) Flavoprotein autofluorescence. **D**) Aggregate:monomer ratios of JC-1. Same letters indicate groups that are not statistically different.

two studies have found increased prevalence of mitochondrial mutations in oocytes from older women [26, 27].

Pdha1⁻ oocytes develop a compromised energetic status as they attempt to complete meiotic maturation, as reflected by total ATP content (Fig. 4A). The inability to metabolize pyruvate impairs mitochondrial metabolism of not only pyruvate but also a number of other energy-producing substrates that are converted to pyruvate, such as glucose, lactate, and a number of amino acids. The decreased NAD(P)H and increased flavoprotein autofluorescence relative to *Pdha1*⁺ oocytes suggests that the energy deficit arises from impaired mitochondrial energy production. The increase in NAD(P)H fluorescence as *Pdha1*⁻ oocytes undergo meiotic maturation may be related to increased production of NADH or NAD(P)H in the cytosol or mitochondria from alternative metabolic pathways. In light of cellular ATP levels of *Pdha1*⁻ oocytes, it is more likely that the increase in NAD(P)H occurs within the cytosol, as oocytes have a reduced ability to convert cytosolic NADH to ATP due to a limited malate-aspartate shuttle [28]. The impressively high flavoprotein fluorescence is likely related to the fact that up to half of the mitochondrial flavoprotein signal comes from DLD, an enzymatic component of PDC and several other multienzyme complexes. In *Pdha1* deficiency, reducing equivalents are not transferred to DLD, thereby causing much of this enzyme to exist in the oxidized, fluorescent form. Why *Pdha1*⁻ oocytes become energetically compromised during meiotic maturation is probably related to two factors: (1) the loss of gap junctional connections with cumulus cells at this stage [29] and (2) the increased energy requirements during this developmental period.

The compromised energy status of *Pdha1*⁻ oocytes may provide an explanation for the observed meiotic defects. Many of the processes involved in meiotic maturation are energy dependent. For instance, chromatin condensation during meiosis is an ATP-dependent process that requires several enzymes from the SMC family of ATPases [30]. Microtubule assembly and chromosomal movement also requires ATP [31]. Thus, the chromatin and microtubular abnormalities in *Pdha1*⁻ oocytes may be a direct consequence of inadequate ATP. Notably, a recent study demonstrated that injury of mitochondria in metaphase II oocytes reduces ATP content and disrupts the meiotic spindle [32]. It also has been shown that mouse and human oocytes with lower total ATP content have diminished developmental potential [33, 34]. Although it is likely that energy deficit plays a central role in the phenotype of *Pdha1*⁻ oocytes, other factors, such as lactic acidosis, meiotic checkpoints, and apoptosis, may contribute to the phenotype. It is well recognized that deficiency in pyruvate dehydrogenase causes lactic acidosis at the cellular and organismal levels [35]. It is possible that follicles containing Pdha1⁻ oocytes develop a localized lactic acidosis due to upregulation of glycolysis in the oocyte and/or granulosa cells. Accumulation of lactate would create an acidic environment that may contribute to the demise of *Pdha1*⁻ oocytes. Developmental arrest of *Pdha1*⁻ oocytes also may arise from failure to complete a meiotic checkpoint, such as proper spindle formation or DNA integrity [36, 37]. The highly condensed chromatin observed in *Pdha1*⁻ oocytes may represent an apoptotic change. Several reports have noted apoptotic nuclear changes in the absence of the two markers of apoptosis examined in this study, double-stranded breaks and alterations in mitochondrial membrane potential [38, 39]. Future studies will attempt to alleviate these meiotic abnormalities by enhancing energy production in *Pdha1*⁻ oocytes during maturation in vitro.

One of the most interesting findings in these studies is that *Pdha1*-deficient oocytes can develop through the entire growth phase, despite inactivation of this enzyme at the beginning of this period. The explanation for continued development of *Pdha1*⁻ oocytes could be related to (1) persistence of gene product, (2) lack of need for this enzyme at earlier developmental stages, or (3) metabolic compensation of the oocyte and/or cumulus cells. The first potential explanation seems unlikely, based on immunohistochemical analyses showing substantially reduced PDH enzyme early in the growth phase (Fig. 1). The second proposed explanation is less plausible, due to previous findings that oocytes collected throughout the growth phase can oxidatively metabolize pyruvate in vitro [4]. The last explanation is most tenable, particularly in light of the results of the in vitro maturation experiments in this study demonstrating that cumulus cells can compensate for this metabolic deficiency (Fig. 3B). Cumulus cells may assist *Pdha1*⁻ oocytes by directly providing ATP or other substrates for energy metabolism via the gap junctional connections. It has been previously shown that oocytes enclosed in cumulus cells have higher amounts of ATP than those lacking cumulus cells [10]. It is likely that the cumulus cells upregulate their metabolism to compensate for the oocyte's increased energetic requirements. A recent study has shown that oocytes can induce an upregulation of glycolysis and oxidative metabolism in cumulus cells by paracrine signaling [40]. It has long been appreciated that granulosa cells are required for proper oocyte growth. This study provides evidence that granulosa cells are even capable of compensating for metabolic impairments in developing oocytes.

The ovulation of *Pdha1*⁻ oocytes is an important observation. It has been proposed that female germ cells with impaired mitochondrial metabolism are selected against at several periods of germ cell development, including the growth phase of oogenesis [41]. The ovulation of *Pdha1*⁻ oocytes demonstrates that metabolically impaired oocytes are not absolutely eliminated during the growth phase. It may be, however, that these oocytes would be selectively eliminated if they were to develop alongside oocytes with normal metabolism, as would be more commonly seen in normal ovarian physiology. At present, it is unclear whether such selection occurs during the growth phase. Without such a selective mechanism, oocytes with impaired mitochondrial metabolism would be ovulated and might account for a subset of oocytes that do not support embryonic development. Oocytes with damaged mitochondria may arise as a result of aging or environmental insult [42, 43].

ACKNOWLEDGMENTS

REFERENCES

1. Wassarman PM, Albertini DF. The mammalian ovum. In: Knobil E, Neill JD (eds.), The Physiology of Reproduction, vol. 1. New York: Raven Press; 1994:79–122.
2. Biggers JD, Whittingham DG, Donahue RP. The pattern of energy metabolism in the mouse oocyte and zygote. Proc Natl Acad Sci U S A 1967; 58:560–567.
3. Brinster RL. Oxidation of pyruvate and glucose by oocytes of the mouse and rhesus monkey. J Reprod Fertil 1971; 24:187–191.
4. Eppig JJ. Analysis of mouse oogenesis in vitro. Oocyte isolation and the utilization of exogenous energy sources by growing oocytes. J Exp Zool 1976; 198:375–382.
5. Zeilmaker GH, Verhamme CM. Observations on rat oocyte maturation in vitro: morphology and energy requirements. Biol Reprod 1974; 11:145–152.
6. Wassarman PM, Josefowicz WJ. Oocyte development in the mouse: an

ultrastructural comparison of oocytes isolated at various stages of growth and meiotic competence. J Morphol 1978; 156:209–235.

7. Boland NI, Gosden RG. Clonal analysis of chimaeric mouse ovaries using DNA in situ hybridization. J Reprod Fertil 1994; 100:203–210.

8. Anderson E, Albertini DF. Gap junctions between the oocyte and companion follicle cells in the mammalian ovary. J Cell Biol 1976; 71: 680–686.

9. Heller DT, Cahill DM, Schultz RM. Biochemical studies of mammalian oogenesis: metabolic cooperativity between granulosa cells and growing mouse oocytes. Dev Biol 1981; 84:455–464.

10. Downs SM. The influence of glucose, cumulus cells, and metabolic coupling on ATP levels and meiotic control in the isolated mouse oocyte. Dev Biol 1995; 167:502–512.

11. Sugiura K, Eppig JJ. Society for Reproductive Biology Founders' Lecture 2005. Control of metabolic cooperativity between oocytes and their companion granulosa cells by mouse oocytes. Reprod Fertil Dev 2005; 17: 667–674.

12. Leese HJ, Barton AM. Production of pyruvate by isolated mouse cumulus cells. J Exp Zool 1985; 234:231–236.

13. Johnson MT, Mahmood S, Hyatt SL, Yang HS, Soloway PD, Hanson RW, Patel MS. Inactivation of the murine pyruvate dehydrogenase (Pdha1) gene and its effect on early embryonic development. Mol Genet Metab 2001; 74:293–302.

14. de Vries WN, Binns LT, Fancher KS, Dean J, Moore R, Kemler R, Knowles BB. Expression of Cre recombinase in mouse oocytes: a means to study maternal effect genes. Genesis 2000; 26:110–112.

15. Lan ZJ, Xu X, Cooney AJ. Differential oocyte-specific expression of Cre recombinase activity in GDF-9-iCre, Zp3cre, and Msx2Cre transgenic mice. Biol Reprod 2004; 71:1469–1474.

16. Hodges CA, Ilagan A, Jennings D, Keri R, Nilson J, Hunt PA. Experimental evidence that changes in oocyte growth influence meiotic chromosome segregation. Hum Reprod 2002; 17:1171–1180.

17. Conover JC, Gwatkin RB. Pre-loading of mouse oocytes with DNA-specific fluorochrome (Hoechst 33342) permits rapid detection of sperm-oocyte fusion. J Reprod Fertil 1988; 82:681–690.

18. van de Sandt JJ, Schroeder AC, Eppig JJ. Culture media for mouse oocyte maturation affect subsequent embryonic development. Mol Reprod Dev 1990; 25:164–171.

19. Debey P, Szollosi MS, Szollosi D, Vautier D, Girousse A, Besombes D. Competent mouse oocytes isolated from antral follicles exhibit different chromatin organization and follow different maturation dynamics. Mol Reprod Dev 1993; 36:59–74.

20. Downs SM. A gap-junction-mediated signal, rather than an external paracrine factor, predominates during meiotic induction in isolated mouse oocytes. Zygote 2001; 9:71–82.

21. Combelles CM, Albertini DF. Assessment of oocyte quality following repeated gonadotropin stimulation in the mouse. Biol Reprod 2003; 68: 812–821.

22. Kunz W, Gellerich FN, Schild L. Contribution to control of mitochondrial oxidative phosphorylation by supplement of reducing equivalents. Biochem Med Metab Biol 1994; 52:65–75.

23. Winkler K, Kuznetsov AV, Lins H, Kirches E, von Bossanyi P, Dietzmann K, Frank B, Feistner H, Kunz WS. Laser-excited fluorescence studies of mitochondrial function in saponin-skinned skeletal muscle fibers of patients with chronic progressive external ophthalmoplegia. Biochim Biophys Acta 1995; 1272:181–184.

24. Reers M, Smith TW, Chen LB. J-aggregate formation of a carbocyanine as a quantitative fluorescent indicator of membrane potential. Biochemistry 1991; 30:4480–4486.

25. Hu CW, Utter MF, Patel MS. Induction of pyruvate dehydrogenase in 3T3-L1 cells during differentiation. J Biol Chem 1983; 258:2315–2320.

26. Brenner CA, Wolny YM, Barritt JA, Matt DW, Munne S, Cohen J. Mitochondrial DNA deletion in human oocytes and embryos. Mol Hum Reprod 1998; 4:887–892.

27. Keefe DL, Niven-Fairchild T, Powell S, Buradagunta S. Mitochondrial deoxyribonucleic acid deletions in oocytes and reproductive aging in women. Fertil Steril 1995; 64:577–583.

28. Lane M, Gardner DK. Mitochondrial malate-aspartate shuttle regulates mouse embryo nutrient consumption. J Biol Chem 2005; 280:18361–18367.

29. Gilula NB, Epstein ML, Beers WH. Cell-to-cell communication and ovulation. A study of the cumulus-oocyte complex. J Cell Biol 1978; 78: 58–75.

30. Hirano T. SMC proteins and chromosome mechanics: from bacteria to humans. Philos Trans R Soc Lond B Biol Sci 2005; 360:507–514.

31. Inoue S, Salmon ED. Force generation by microtubule assembly/disassembly in mitosis and related movements. Mol Biol Cell 1995; 6: 1619–1640.

32. Zhang X, Wu XQ, Lu S, Guo YL, Ma X. Deficit of mitochondria-derived ATP during oxidative stress impairs mouse MII oocyte spindles. Cell Res 2006; 16:841–850.

33. Igarashi H, Takahashi T, Takahashi E, Tezuka N, Nakahara K, Takahashi K, Kurachi H. Aged mouse oocytes fail to readjust intracellular adenosine triphosphates at fertilization. Biol Reprod 2005; 72:1256–1261.

34. Van Blerkom J, Davis PW, Lee J. ATP content of human oocytes and developmental potential and outcome after in-vitro fertilization and embryo transfer. Hum Reprod 1995; 10:415–424.

35. Robinson BH. Lactic acidemia: disorders of pyruvate carboxylase and pyruvate dehydrogenase. In: Scriver CR, Beaudet AL, Sly WS, Valle D (eds.), The Metabolic and Molecular Bases of Inherited Disease, vol. 2. New York: McGraw-Hill; 2001:2275–2295.

36. Steuerwald N. Meiotic spindle checkpoints for assessment of aneuploid oocytes. Cytogenet Genome Res 2005; 111:256–259.

37. Liu L, Trimarchi JR, Smith PJ, Keefe DL. Checkpoint for DNA integrity at the first mitosis after oocyte activation. Mol Reprod Dev 2002; 62:277–288.

38. Sakahira H, Enari M, Ohsawa Y, Uchiyama Y, Nagata S. Apoptotic nuclear morphological change without DNA fragmentation. Curr Biol 1999; 9:543–546.

39. Ly JD, Grubb DR, Lawen A. The mitochondrial membrane potential (deltapsi(m)) in apoptosis; an update. Apoptosis 2003; 8:115–128.

40. Sugiura K, Pendola FL, Eppig JJ. Oocyte control of metabolic cooperativity between oocytes and companion granulosa cells: energy metabolism. Dev Biol 2005; 279:20–30.

41. Krakauer DC, Mira A. Mitochondria and germ-cell death. Nature 1999; 400:125–126.

42. Kovacic P, Pozos RS, Somanathan R, Shangari N, O'Brien PJ. Mechanism of mitochondrial uncouplers, inhibitors, and toxins: focus on electron transfer, free radicals, and structure-activity relationships. Curr Med Chem 2005; 12:2601–2623.

43. Ozawa T. Genetic and functional changes in mitochondria associated with aging. Physiol Rev 1997; 77:425–464.